

# Polarizations of $\chi_{c1}$ and $\chi_{c2}$ in Prompt Production at the LHC

Hua-Sheng Shao<sup>(a)</sup>, Yan-Qing Ma<sup>(b)</sup>, Kai Wang<sup>(a)</sup>, Kuang-Ta Chao<sup>(a,c,d)</sup>

(a) School of Physics and State Key Laboratory of Nuclear Physics and Technology, Peking University, Beijing 100871, China

(b) Physics Department, Brookhaven National Laboratory, Upton, NY 11973, USA

(c) Collaborative Innovation Center of Quantum Matter, Beijing 100871, China

(d) Center for High Energy Physics, Peking University, Beijing 100871, China

Prompt  $\chi_c$  production at hadron colliders may provide a unique test for the color-octet mechanism in nonrelativistic QCD. We present an analysis for the polarization observables of  $\chi_{c1}$  and  $\chi_{c2}$  at next-to-leading order in  $\alpha_S$ , and propose to measure them at the LHC, which is expected to be important for testing the validity of NRQCD.

PACS numbers: 12.38.Bx, 13.60.Le, 13.88.+e, 14.40.Pq

Heavy quarkonium production provides an ideal laboratory to understand quantum chromodynamics. In contrast to the helicity-summed cross section, the quarkonium polarization measurement may provide more complete information for the production mechanism of heavy quarkonium [1].

A distinct example is the  $J/\psi$  polarization at hadron colliders. The polar asymmetry coefficient  $\lambda_\theta$  in the angular distribution of the leptons from the  $J/\psi$  decay is an important observable that encodes the  $J/\psi$  polarization information. At the Tevatron, the CDF Collaboration measured the quantity many years ago [2, 3]. Their measurements show that  $\lambda_\theta$  for prompt  $J/\psi$  production in its helicity frame is around zero up to  $p_T = 30\text{GeV}$ , indicating that the  $J/\psi$  mesons are produced in the unpolarized pattern. The state-of-the-art theory that describes the heavy quarkonium dynamics, non-relativistic QCD (NRQCD) [4], predicts that the heavy quark pair is allowed to be created in a color-octet (CO) intermediate state at short distances and then evolves nonperturbatively into a color-singlet (CS) quarkonium at long distances. Although this CO mechanism provides an opportunity to account for the CDF yield data [5, 6] that cannot be resolved in the CS model (CSM) even by including the higher-order QCD corrections [7, 8], the leading-order (LO) in  $\alpha_S$  NRQCD prediction gives a completely transverse polarization result at high  $p_T$  due to gluon fragmentation to the CO  $^3S_1^{[8]}$  intermediate state [9]. Recently, three groups reported their next-to-leading order (NLO) QCD corrections to the  $J/\psi$  polarization [10–12]. Recall that the  $J/\psi$  polarization is strongly dependent on the specific choice of the nonperturbative long-distance matrix elements (LDMEs), which can only be determined from the experimental data. Choosing different  $p_T$  regions of the input experimental data may result in very different predictions. Therefore, the precise measurement of polarization, especially at high  $p_T$ , may provide a smoking-gun signature to distinguish between various production mechanisms of heavy quarkonium. Moreover, it was pointed out in Ref.[11] that there is still a CO LDMEs parameter space left to make both the helicity-

summed yields and  $\lambda_\theta$  quite satisfactory compared to the hadroproduction data.

However, the prompt  $J/\psi$  production at the Tevatron and LHC is affected substantially by the higher charmonia (e.g.  $\chi_c$  and  $\psi'$ ) transitions to  $J/\psi$ . Furthermore, even for direct  $J/\psi$  production there are three leading CO LDMEs, which makes the precise determination of CO LDMEs difficult. In contrast, for the  $\chi_c$  hadroproduction the feed-down contribution only comes from  $\psi'$  to  $\chi_c$  transition, but they are not significant, and there is only one leading CO state  $^3S_1^{[8]}$  involving  $\chi_c$  direct production, which can make the determination of the LDMEs easier and more precise. Moreover, the higher-order QCD corrections to the conventional P-wave CS state suffer from severe infrared divergences, while in NRQCD these divergences can be absorbed by the CO state and, thus, make the P-wave observables well defined beyond LO. Given these reasons, the investigation of  $\chi_c$  production at the LHC is an important way to test the validity of NRQCD factorization and the CO mechanism.

The first investigation for the helicity-summed  $\chi_c$  hadroproduction at NLO level was performed in Ref.[13]. In this Letter, we extend our calculation to the polarized case, with the method described in Refs.[11, 14]. The polarization observables of  $\chi_{c1}$  and  $\chi_{c2}$  were proposed in Refs.[15–17]. Experimentally, one may have two ways to measure the polarization of  $\chi_{c1}$  and  $\chi_{c2}$  through the angular distributions of their decay products. One is to measure the  $J/\psi$  angular distribution from  $\chi_c \rightarrow J/\psi\gamma$ . The angular distribution with respect to the  $J/\psi$  polar angle  $\theta$  in the rest frame of  $\chi_c$  can be formulated as [17]

$$\frac{d\mathcal{N}_{\chi_{cJ}}}{d\cos\theta} \propto 1 + \sum_{k=1}^J \lambda_{k\theta} \cos^{2k}\theta, \quad (1)$$

where the polar asymmetry coefficients  $\lambda_{k\theta}$  can be expressed as the rational functions of the  $\chi_{cJ}$  production spin density matrix  $\rho^{\chi_{cJ}}$ . More specifically, for  $\chi_{c1}$  it is

$$\lambda_\theta = (1 - 3\delta) \frac{N_{\chi_{c1}} - 3\rho_{0,0}^{\chi_{c1}}}{(1 + \delta)N_{\chi_{c1}} + (1 - 3\delta)\rho_{0,0}^{\chi_{c1}}}, \quad (2)$$

with  $N_{\chi_{c1}} \equiv \rho_{1,1}^{\chi_{c1}} + \rho_{0,0}^{\chi_{c1}} + \rho_{-1,-1}^{\chi_{c1}}$ , whereas for  $\chi_{c2}$ , the coefficients are

$$\begin{aligned}\lambda_\theta &= 6[(1 - 3\delta_0 - \delta_1)N_{\chi_{c2}} \\ &\quad - (1 - 7\delta_0 + \delta_1)(\rho_{1,1}^{\chi_{c2}} + \rho_{-1,-1}^{\chi_{c2}}) \\ &\quad - (3 - \delta_0 - 7\delta_1)\rho_{0,0}^{\chi_{c2}}]/R, \\ \lambda_{2\theta} &= (1 + 5\delta_0 - 5\delta_1)[N_{\chi_{c2}} - 5(\rho_{1,1}^{\chi_{c2}} + \rho_{-1,-1}^{\chi_{c2}}) \\ &\quad + 5\rho_{0,0}^{\chi_{c2}}]/R,\end{aligned}\quad (3)$$

with

$$\begin{aligned}N_{\chi_{c2}} &= \rho_{2,2}^{\chi_{c2}} + \rho_{1,1}^{\chi_{c2}} + \rho_{0,0}^{\chi_{c2}} + \rho_{-1,-1}^{\chi_{c2}} + \rho_{-2,-2}^{\chi_{c2}}, \\ R &= (1 + 5\delta_0 + 3\delta_1)N_{\chi_{c2}} \\ &\quad + 3(1 - 3\delta_0 - \delta_1)(\rho_{1,1}^{\chi_{c2}} + \rho_{-1,-1}^{\chi_{c2}}) \\ &\quad + (5 - 7\delta_0 - 9\delta_1)\rho_{0,0}^{\chi_{c2}}.\end{aligned}$$

The parameters  $\delta$ ,  $\delta_0$  and  $\delta_1$  can be determined by the normalized multipole amplitudes. Following the notations in Ref.[18], we denote the normalized electric dipole (E1) transition amplitudes by  $a_1^{J=1}$  and  $a_1^{J=2}$  for  $\chi_{c1}$  and  $\chi_{c2}$ , respectively, while  $a_2^{J=1}$ ,  $a_2^{J=2}$ ,  $a_3^{J=2}$  are the  $\chi_{c1}$  and  $\chi_{c2}$  normalized magnetic quadrupole (M2) amplitudes and  $\chi_{c2}$  electric octupole amplitude (E3). We remind readers that the word “normalized” here means we have relations  $a_1^{J=1} + a_2^{J=1} = 1$  and  $a_1^{J=2} + a_2^{J=2} + a_3^{J=2} = 1$ . The explicit expressions for  $\delta$ ,  $\delta_0$ ,  $\delta_1$  are

$$\begin{aligned}\delta &= (1 + 2a_1^{J=1}a_2^{J=1})/2, \\ \delta_0 &= [1 + 2a_1^{J=2}(\sqrt{5}a_2^{J=2} + 2a_3^{J=2}) \\ &\quad + 4a_2^{J=2}(a_2^{J=2} + \sqrt{5}a_3^{J=2}) + 3(a_3^{J=2})^2]/10, \\ \delta_1 &= [9 + 6a_1^{J=2}(\sqrt{5}a_2^{J=2} - 4a_3^{J=2}) \\ &\quad - 4a_2^{J=2}(a_2^{J=2} + 2\sqrt{5}a_3^{J=2}) + 7(a_3^{J=2})^2]/30.\end{aligned}\quad (4)$$

An alternative way to study the polarizations of  $\chi_{c1}$  and  $\chi_{c2}$  is to measure the dilepton angular distributions from  $\chi_{cJ} \rightarrow J/\psi \gamma \rightarrow l^+ l^- \gamma$ . There are two choices to describe the dilepton angular distributions [16, 17]. Here, we only choose the second one presented in Ref.[17], where the  $z$  axis in the rest frame of  $J/\psi$  coincides with the direction of the spin quantization axis in the  $\chi_c$  rest frame. The generic lepton polar angle  $\theta'$  dependence is

$$\frac{d\mathcal{N}^{\chi_{cJ}}}{d\cos\theta'} \propto 1 + \lambda_{\theta'} \cos^2\theta', \quad (5)$$

where

$$\begin{aligned}\lambda_{\theta'}^{\chi_{c1}} &= \frac{-N_{\chi_{c1}} + 3\rho_{0,0}^{\chi_{c1}}}{R_1}, \\ \lambda_{\theta'}^{\chi_{c2}} &= \frac{6N_{\chi_{c2}} - 9(\rho_{1,1}^{\chi_{c2}} + \rho_{-1,-1}^{\chi_{c2}}) - 12\rho_{0,0}^{\chi_{c2}}}{R_2},\end{aligned}\quad (6)$$

with

$$\begin{aligned}R_1 &= [(15 - 2(a_2^{J=1})^2)N_{\chi_{c1}} \\ &\quad - (5 - 6(a_2^{J=1})^2)\rho_{0,0}^{\chi_{c1}}]/(5 - 6(a_2^{J=1})^2), \\ R_2 &= [2(21 + 14(a_2^{J=2})^2 + 5(a_3^{J=2})^2)N_{\chi_{c2}} \\ &\quad + 3(7 - 14(a_2^{J=2})^2 - 5(a_3^{J=2})^2)(\rho_{1,1}^{\chi_{c2}} + \rho_{-1,-1}^{\chi_{c2}}) \\ &\quad + 4(7 - 14(a_2^{J=2})^2 - 5(a_3^{J=2})^2)\rho_{0,0}^{\chi_{c2}}] \\ &\quad \div [7 - 14(a_2^{J=2})^2 - 5(a_3^{J=2})^2].\end{aligned}$$

Note that  $\lambda_{2\theta}$  for  $\chi_{c2}$  is suppressed by the higher-order multipole amplitudes  $a_2^{J=2}, a_3^{J=2}$ . The observable is expected to be near zero. Hence, we refrain from establishing the  $p_T$  distribution of  $\lambda_{2\theta}$  here.

In our numerical computation, we choose the same input parameters as those presented in Ref.[11]. The renormalization scale  $\mu_r$ , factorization scales  $\mu_f$  and NRQCD scale  $\mu_\Lambda$  are chosen as  $\mu_r = \mu_f = \sqrt{4m_c^2 + p_T^2}$  and  $\mu_\Lambda = m_c$ . The CO LDMEs are chosen to be  $\langle \mathcal{O}^{\chi_{cJ}}(^3S_1^{[8]}) \rangle = (2J+1) \times (2.2_{-0.32}^{+0.48}) \times 10^{-3} \text{GeV}^3$  [13], which are obtained by fitting the ratio  $\sigma_{\chi_{c2}}/\sigma_{\chi_{c1}}$  at NLO level to the CDF data [19], while the CS LDMEs are estimated using the B-T potential model [20] as  $\langle \mathcal{O}(^3P_J^{[1]}) \rangle = (2J+1)[(3|R'(0)|^2)/4\pi]$  with  $|R'(0)|^2 = 0.075 \text{GeV}^5$ . The uncertainties due to the scale dependence, which is estimated by varying  $\mu_r, \mu_f$  by a factor of  $\frac{1}{2}$  to 2 with respect to their central values, the charm quark mass  $m_c = 1.5 \pm 0.1 \text{GeV}$  and the error in the CDF data [19] are all encoded in the error estimations of the CO LDMEs. The normalized multipole amplitudes used here are taken from the CLEO measurement [18], i.e.  $a_2^{J=1} = (-6.26 \pm 0.68) \times 10^{-2}$ ,  $a_2^{J=2} = (-9.3 \pm 1.6) \times 10^{-2}$ ,  $a_3^{J=2} = 0$ . We keep the E3 amplitude  $a_3^{J=2}$  vanishing, which is the consequence of the single quark radiation hypothesis [21, 22].

As was done in Ref.[13], we have tried to improve the uncertainties in the ratio  $r \equiv m_c^2 \langle \mathcal{O}^{\chi_{c0}}(^3S_1^{[8]}) \rangle / \langle \mathcal{O}^{\chi_{c0}}(^3P_0^{[1]}) \rangle$  by using the LHCb data [23] and CMS data [26]. With the Tevatron data, it was determined to be  $r = 0.27 \pm 0.06$ . But its accuracy is not improved significantly with the updated LHC data. With the LHCb data [23],  $r$  varies from 0.35 to 0.31 when using a different  $p_T$  cutoff. (To be compatible with our  $J/\psi$  case [11], we always ignore the data when  $p_T < 7 \text{GeV}$ .) Using the CMS data [26], we find  $r$  has very weak dependence on  $p_T$  cutoff, and its value is almost 0.25 with unpolarized hypothesis. The substantial uncertainty in the  $r$  extraction is due to different polarisation hypotheses. The  $r$  value changes from 0.21 to 0.31 in two extreme hypotheses [26]. Therefore, it is acceptable for us to choose  $r = 0.27 \pm 0.06$  here. Here, we may choose  $r = 0.27 \pm 0.06$  as an acceptable value, and the value of  $r$  from different extractions are well embodied in its uncertainties. We emphasize further that measurements with higher resolution, especially in the high  $p_T$  region, will be very useful to improve our NRQCD predictions.

In Fig.1, the cross section ratios  $\sigma_{\chi_{c2}}/\sigma_{\chi_{c1}}$  at the

Tevatron Run II and LHC are shown. For comparison, besides the NLO NRQCD predictions, we also plot the LO NRQCD results and the LO CSM results. We see the NLO NRQCD results are consistent with the CDF data [19] and the CMS data [26] in the whole  $p_T^{J/\psi}$  region, while in the forward rapidity region the NLO NRQCD prediction is in agreement with the LHCb data [23] only when  $p_T^{J/\psi} > 8\text{GeV}$ , which may imply that some unknown nonperturbative effects make our fixed-order results unreliable when  $p_T^{J/\psi}$  is lower. Note that  $p_T^{J/\psi}$  is obtained from  $p_T$  of  $\chi_c$  by the mass rescaling  $p_T^{J/\psi} = \frac{m_{J/\psi}}{m_{\chi_c J}} p_T$ , which is proven to be a good approximation by the Monte Carlo simulation. Here the masses  $m_{J/\psi} = 3.10\text{GeV}$ ,  $m_{\chi_{c1}} = 3.51\text{GeV}$ ,  $m_{\chi_{c2}} = 3.56\text{GeV}$ , and branching ratios  $\text{Br}(\chi_{c1} \rightarrow J/\psi\gamma) = 0.344$ ,  $\text{Br}(\chi_{c2} \rightarrow J/\psi\gamma) = 0.195$  are taken from Ref.[24]. We see also that the LO CSM prediction is substantially lower than the experimental data. Two other important obstacles for CSM are the measured cross section of  $\chi_{cJ}$  at the Tevatron Run I [13] and ratio  $\sigma(\chi_{cJ} \rightarrow J/\psi\gamma)/\sigma(J/\psi)$  at the LHC [25]. While there are discrepancies between the LO CSM predictions and the experimental data, the NLO NRQCD results are reasonably good. To present the predictions of the cross sections at the LHC, we also show the corresponding curves in Fig.3. In Fig.2, we present the curves of spin density matrix elements  $d\sigma_{00}/dp_T$ ,  $d\sigma_{11}/dp_T$  (and  $d\sigma_{22}/dp_T$ ) for  $\chi_{c1}(\chi_{c2})$  with  $\sqrt{s} = 7\text{ TeV}$  and  $|y| < 2.4$ . To be more specific, we also show curves in different Fock states( with LDMEs given above ). The negative values (see also Refs.[10–12]) are marked red.

TABLE I: Upper and lower bound values of the observables  $\lambda_\theta$  and  $\lambda_{\theta'}$  for  $\chi_{c1}$  and  $\chi_{c2}$ .

Observable	$\lambda_\theta^{\chi_{c1}}$	$\lambda_\theta^{\chi_{c2}}$	$\lambda_{\theta'}^{\chi_{c1}}$	$\lambda_{\theta'}^{\chi_{c2}}$
Upper bound	0.556	1.61	0.994	0.928
Lower bound	-0.217	-0.803	-0.332	-0.574

For the numerical results of the polarization observables of  $\chi_{c1}$  and  $\chi_{c2}$ , we use expressions in Eqs.(2,3, and 6) and obtain , first, the lower and upper bound val-

ues of  $\lambda_\theta$  and  $\lambda_{\theta'}$  for  $\chi_c$  regardless of its production mechanisms. They are presented in Table I. When  $\rho_{1,1}^{\chi_{c1}} = \rho_{-1,-1}^{\chi_{c1}} \ll \rho_{0,0}^{\chi_{c1}}$ , the polar observables for  $\chi_{c1}$  approach their maximal values, whereas the minimal values are obtained when  $\rho_{1,1}^{\chi_{c1}} = \rho_{-1,-1}^{\chi_{c1}} \gg \rho_{0,0}^{\chi_{c1}}$ . For  $\chi_{c2}$ , the polar asymmetry coefficients  $\lambda_\theta$  and  $\lambda_{\theta'}$  are maximum when  $\rho_{2,2}^{\chi_{c2}} = \rho_{-2,-2}^{\chi_{c2}} \gg \rho_{1,1}^{\chi_{c2}} = \rho_{-1,-1}^{\chi_{c2}}, \rho_{0,0}^{\chi_{c2}}$  and minimum when  $\rho_{2,2}^{\chi_{c2}} = \rho_{-2,-2}^{\chi_{c2}}, \rho_{1,1}^{\chi_{c2}} = \rho_{-1,-1}^{\chi_{c2}} \ll \rho_{0,0}^{\chi_{c2}}$ . The  $p_T$  distributions of  $\lambda_\theta$  and  $\lambda_{\theta'}$  are shown in Figs. 4 and 5, respectively. It is worth noting that the transformation relation between the spin density matrices of  $^3S_1^{[8]}$  and those of  $^3P_J^{[1]}$  [17]

$$\rho_{J_z, J_z'}^{^3S_1^{[8]} \rightarrow \chi_{cJ}} \propto \sum_{l_z, s_z, s_z' = \pm 1, 0} \rho_{s_z, s_z'}^{^3S_1^{[8]}} \times \langle 1, l_z; 1, s_z | J, J_z \rangle \langle 1, l_z; 1, s_z' | J, J_z' \rangle, \quad (7)$$

is used in our numerical results. The error bands in these figures are due to uncertainties of the CO LDMEs  $\langle \mathcal{O}^{\chi_{cJ}}(^3S_1^{[8]}) \rangle$  and errors in the normalized multipole amplitudes. From Figs.4 and 5, we see that the measurements of these polarization observables may provide another important way to test the CO mechanism in the hadroproduction of heavy quarkonium.

In summary, we have performed an analysis of the polarized  $\chi_{c1}$  and  $\chi_{c2}$  production at the LHC in NRQCD and in the color-singlet model. The complete NLO NRQCD predictions are given for the first time. These observables may provide important information, which is not available in the helicity-summed  $p_T$  spectra, in testing the validity of NRQCD factorization. Compared with  $J/\psi$  production, the prompt  $\chi_c$  production may play a unique role in understanding the heavy quarkonium production mechanism. Therefore, we propose to measure these polarization observables at the LHC.

We are grateful to C. Meng, Y.J. Zhang and H. Han for helpful discussions. This work was supported in part by the National Natural Science Foundation of China (Nos.11021092,11075002). Y.-Q.M is supported by the U.S. Department of Energy, contract number DE-AC02-98CH10886.

- 
- [1] N. Brambilla *et al.*, “Heavy quarkonium: progress, puzzles, and opportunities,” *Eur.Phys.J.* **C71** (2011) 1534, 1010.5827.
- [2] **CDF Collaboration**, T. Affolder *et al.*, “Measurement of  $J/\psi$  and  $\psi(2S)$  polarization in  $p\bar{p}$  collisions at  $\sqrt{s} = 1.8\text{ TeV}$ ,” *Phys.Rev.Lett.* **85** (2000) 2886–2891, hep-ex/0004027.
- [3] **CDF Collaboration**, A. Abulencia *et al.*, “Polarization of  $J/\psi$  and  $\psi_{2S}$  mesons produced in  $p\bar{p}$  collisions at  $\sqrt{s} = 1.96\text{-TeV}$ ,” *Phys.Rev.Lett.* **99** (2007) 132001, 0704.0638.
- [4] G. T. Bodwin, E. Braaten, and G. Lepage, “Rigorous QCD analysis of inclusive annihilation and production of heavy quarkonium,” *Phys.Rev.* **D51** (1995) 1125–1171, hep-ph/9407339.
- [5] **CDF Collaboration**, F. Abe *et al.*, “ $J/\psi$  and  $\psi(2S)$  production in  $p\bar{p}$  collisions at  $\sqrt{s} = 1.8\text{ TeV}$ ,” *Phys.Rev.Lett.* **79** (1997) 572–577.
- [6] **CDF Collaboration**, F. Abe *et al.*, “Production of  $J/\psi$  mesons from  $\chi_c$  meson decays in  $p\bar{p}$  collisions at  $\sqrt{s} = 1.8\text{ TeV}$ ,” *Phys.Rev.Lett.* **79** (1997) 578–583.
- [7] J. M. Campbell, F. Maltoni, and F. Tramontano, “QCD corrections to  $J/\psi$  and Upsilon production at hadron colliders,” *Phys.Rev.Lett.* **98** (2007) 252002, hep-ph/0703113.
- [8] J. Lansberg, “On the mechanisms of heavy-quarkonium

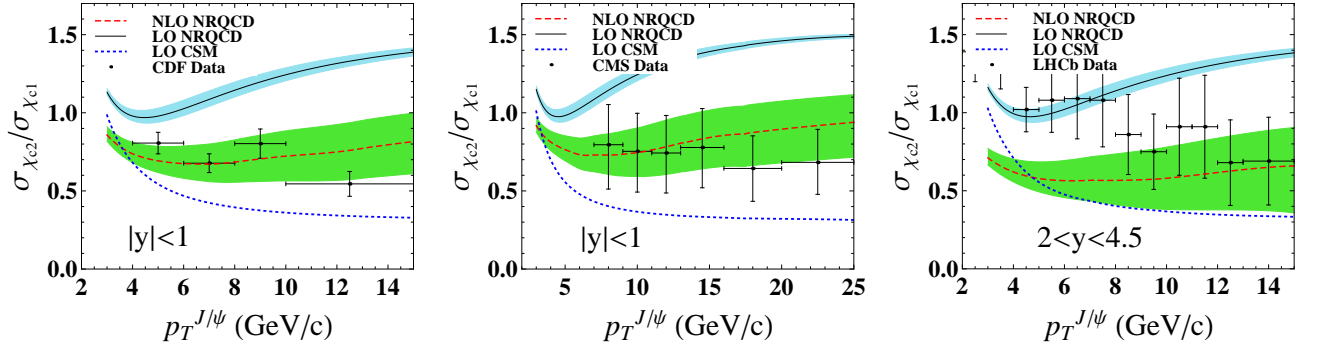


FIG. 1: (color online) The cross-section ratio  $\sigma_{\chi_{c2}}/\sigma_{\chi_{c1}}$  vs the transverse momentum  $p_T^{J/\psi}$  at the Tevatron Run II (left panel) and LHC at  $\sqrt{S} = 7\text{TeV}$  (right two panels). The rapidity cuts are the same as in the experiments [19, 23, 26]. Results for LO NRQCD (solid line), NLO NRQCD (dashed line) and LO CSM (dotted line) are shown.

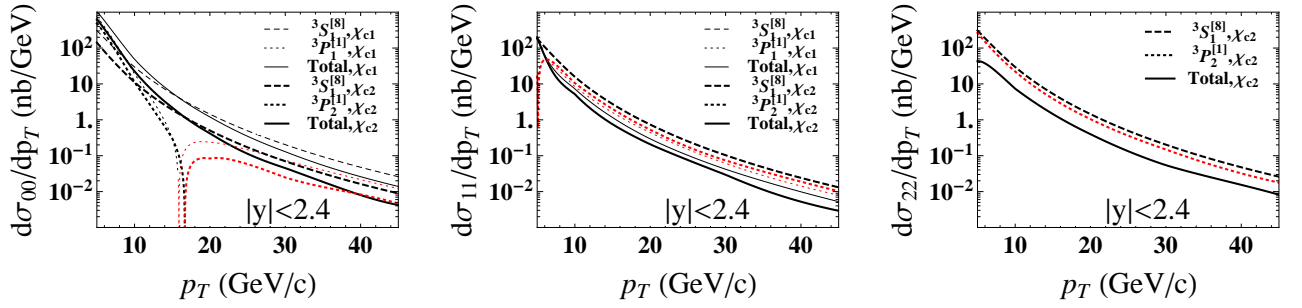


FIG. 2: (color online)  $d\sigma_{00}/dp_T, d\sigma_{11}/dp_T, d\sigma_{22}/dp_T$  for  $pp \rightarrow \chi_{cJ} + X (J = 1, 2)$  with  $\sqrt{S} = 7\text{ TeV}$  and  $|y| < 2.4$  in the helicity frame at NLO in NRQCD. The thin lines represent for  $\chi_{c1}$  whereas the thick lines represent for  $\chi_{c2}$ . Negative values are marked red (lighter).

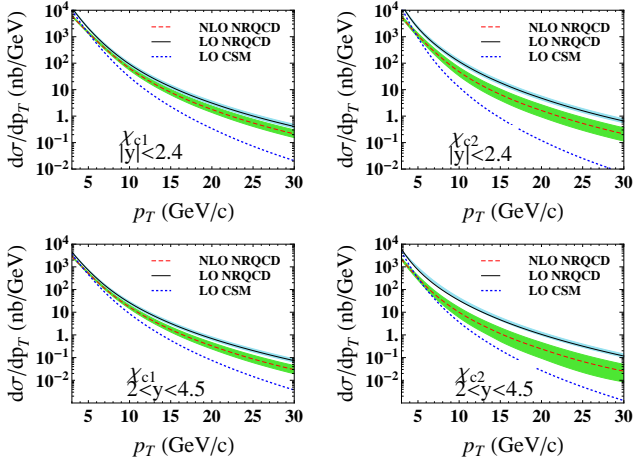


FIG. 3: (color online) Predictions of  $p_T$  spectra for the helicity-summed  $\chi_{c1}$  (left column) and  $\chi_{c2}$  (right column) at the LHC with  $\sqrt{S} = 7\text{TeV}$ . Cross sections in the central rapidity region ( $|y| < 2.4$ ) and forward rapidity region ( $2 < y < 4.5$ ) for  $\chi_c$  are plotted. Results for LO NRQCD (solid line), NLO NRQCD (dashed line) and LO CSM (dotted line) are shown.

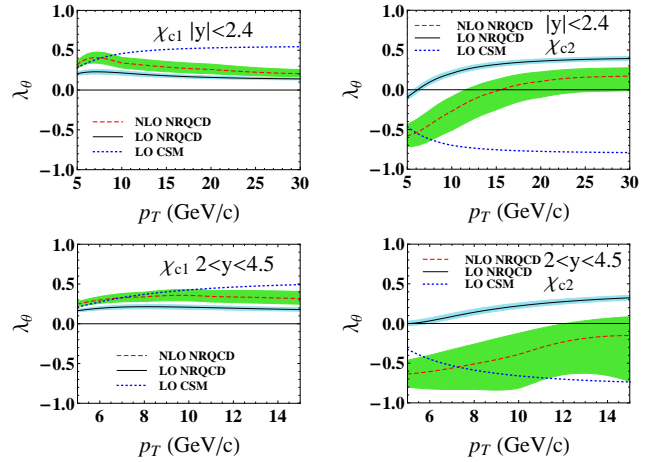


FIG. 4: (color online) The  $p_T$  dependence of  $\lambda_\theta$  with  $J/\psi$  angular distributions from radiative decays  $\chi_{c1} \rightarrow J/\psi\gamma$  (left column) and  $\chi_{c2} \rightarrow J/\psi\gamma$  (right column) in the helicity frame at the LHC with  $\sqrt{S} = 7\text{TeV}$ . Results in central and forward rapidity regions are plotted. The LO NRQCD (solid line), NLO NRQCD (dashed line), and LO CSM (dotted line) predictions are shown.



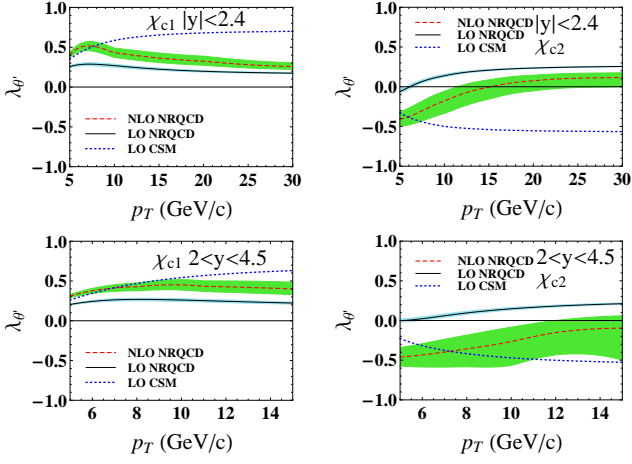


FIG. 5: (color online) The  $p_T$  dependence of  $\lambda_{\theta'}$  with dilepton angular distributions from cascade decays  $\chi_{c1} \rightarrow J/\psi\gamma \rightarrow l^+l^-\gamma$  (left column) and  $\chi_{c2} \rightarrow J/\psi\gamma \rightarrow l^+l^-\gamma$  (right column) in the helicity frame at the LHC with  $\sqrt{S} = 7\text{TeV}$ . Results in central rapidity and forward rapidity regions are plotted, and the LO NRQCD (solid line), NLO NRQCD (dashed line) and LO CSM (dotted line) predictions are shown.

hadroproduction,” *Eur.Phys.J.* **C61** (2009) 693–703, 0811.4005.

- [9] E. Braaten, B. A. Kniehl, and J. Lee, “Polarization of prompt  $J/\psi$  at the Tevatron,” *Phys.Rev.* **D62** (2000) 094005, hep-ph/9911436.
- [10] M. Butenschoen and B. A. Kniehl, “ $J/\psi$  polarization at Tevatron and LHC: Nonrelativistic-QCD factorization at the crossroads,” *Phys.Rev.Lett.* **108** (2012) 172002, 1201.1872.
- [11] K.-T. Chao, Y.-Q. Ma, H.-S. Shao, K. Wang, and Y.-J. Zhang, “ $J/\psi$  polarization at hadron colliders in nonrelativistic QCD,” *Phys.Rev.Lett.* **108** (2012) 242004, 1201.2675.
- [12] B. Gong, L.-P. Wan, J.-X. Wang, and H.-F. Zhang, “Polarization for Prompt  $J/\psi$ ,  $\psi(2s)$  production at the Tevatron and LHC,” *Phys.Rev.Lett.* **110** (2013) 042002, 1205.6682.
- [13] Y.-Q. Ma, K. Wang, and K.-T. Chao, “QCD radiative corrections to  $\chi_{cJ}$  production at hadron colliders,” *Phys.Rev.* **D83** (2011) 111503, 1002.3987.
- [14] H.-S. Shao, “HELAC-Onia: An automatic matrix element generator for heavy quarkonium physics,” *Comput.Phys.Commun.* **184** (2013) 2562–2570, 1212.5293.
- [15] B. A. Kniehl, G. Kramer, and C. P. Palisoc, “ $\chi(c1)$  and  $\chi(c2)$  decay angular distributions at the Fermilab Tevatron,” *Phys.Rev.* **D68** (2003) 114002, hep-ph/0307386.
- [16] P. Faccioli, C. Lourenco, J. Seixas, and H. K. Wohri, “Determination of  $\chi_c$  and  $\chi_b$  polarizations from dilepton angular distributions in radiative decays,” *Phys.Rev.* **D83** (2011) 096001, 1103.4882.
- [17] H.-S. Shao and K.-T. Chao, “Spin correlations in polarizations of P-wave charmonia  $\chi_{cJ}$  and impact on  $J/\psi$  polarization,” 1209.4610.
- [18] **CLEO Collaboration**, M. Artuso *et al.*, “Higher-order multipole amplitudes in charmonium radiative transitions,” *Phys.Rev.* **D80** (2009) 112003, 0910.0046.
- [19] **CDF Collaboration**, A. Abulencia *et al.*, “Measurement of  $\sigma_{\chi_{c2}}\mathcal{B}(\chi_{c2} \rightarrow J/\psi\gamma)/\sigma_{\chi_{c1}}\mathcal{B}(\chi_{c1} \rightarrow J/\psi\gamma)$  in  $p\bar{p}$  collisions at  $\sqrt{s} = 1.96\text{-TeV}$ ,” *Phys.Rev.Lett.* **98** (2007) 232001, hep-ex/0703028.
- [20] E. J. Eichten and C. Quigg, “Quarkonium wave functions at the origin,” *Phys.Rev.* **D52** (1995) 1726–1728, hep-ph/9503356.
- [21] G. Karl, S. Meshkov, and J. L. Rosner, “QUARK MAGNETIC MOMENTS AND E1 RADIATIVE TRANSITIONS IN CHARMONIUM,” *Phys.Rev.Lett.* **45** (1980) 215.
- [22] M. Olsson, I. Suchyta, C.J., A. D. Martin, and W. J. Stirling, “TESTING THE SINGLE QUARK RADIATION HYPOTHESIS,” *Phys.Rev.* **D31** (1985) 1759.
- [23] **LHCb Collaboration**, R. Aaij *et al.*, “Measurement of the cross-section ratio  $\sigma(\chi_{c2})/\sigma(\chi_{c1})$  for prompt  $\chi_c$  production at  $\sqrt{s} = 7\text{ TeV}$ ,” *Phys.Lett.* **B714** (2012) 215–223, 1202.1080.
- [24] **Particle Data Group**, K. Nakamura *et al.*, “Review of particle physics,” *J.Phys.G* **G37** (2010) 075021.
- [25] **LHCb Collaboration**, R. Aaij *et al.*, “Measurement of the ratio of prompt  $\chi_c$  to  $J/\psi$  production in  $pp$  collisions at  $\sqrt{s} = 7\text{ TeV}$ ,” *Phys.Lett.* **B718** (2012) 431–440, 1204.1462.
- [26] **CMS Collaboratin**, S. Chatrchyan *et al.*, “Measurement of the relative prompt production rate of  $\chi(c2)$  and  $\chi(c1)$  in  $pp$  collisions at  $\sqrt{s} = 7\text{ TeV}$ ,” *Eur. Phys. J.* **C72** (2012) 2251, 1210.0875.